Load bus inertia estimation in electrical power networks using distance measurements: a data-driven approach

JUAN M. RAMIREZ*, ALEXANDER SANCHEZ OCAMPO

Department of Electrical Engineering,
Center for Research and Advanced Studies,
Center for Research and Advanced Studies, Zapopan, 45019, Jalisco, MEXICO
*Corresponding author

Abstract: - The integration of renewable energy into power systems reduces grid inertia, posing a stability challenge as inverter-based resources increasingly displace traditional synchronous generators. Accurate inertia estimation, which accounts for contributions from both generator and load inertia, is essential for effective frequency control. Although load inertia is typically smaller than that of generators, its role in dampening frequency fluctuations remains critical. This study applies momentum conservation principles to calculate equivalent load inertia within power networks, yielding findings that validate the proposed method and provide valuable insights for maintaining grid reliability during the transition to renewable energy.

Furthermore, the paper presents a graph-theoretic approach for regional frequency assessment, integrating spectral centrality with an enhanced label propagation technique to identify centres of inertia (COIs) and delineate system communities. By evaluating generator locations and line admittances, the framework partitions networks into coherent clusters, which represent a valuable tool for enabling precise localisation of regional COIs (RCOIs).

Key-Words: - frequency control, inertia estimation, load bus inertia, momentum conservation, power systems stability, and transient stability.

Received: May 25, 2024. Revised: January 14, 2025. Accepted: March 16, 2025. Published: June 16, 2025.

1 Introduction

Modern power systems are facing increasing challenges in frequency stability due to the integration of renewable energy sources and fluctuations in demand, necessitating the development of advanced monitoring solutions [1]. A critical issue is the accurate assessment of regional frequency, which remains hindered by measurement constraints, communication delays, and difficulties in inertia estimation [2]. Traditional approaches—such as interarea oscillation analysis [3], ARMAX methods [4], and swing equations [5]—struggle to precisely locate the centre of inertia (COI), despite its fundamental role in stability [6].

Existing techniques often rely on extensive phasor measurement unit (PMU) deployments, which can introduce inconsistencies [7]. Meanwhile, COI misplacement compromises the rate-of-change-of-frequency (RoCoF) accuracy [8]. Clustering algorithms, though widely used, present limitations: centroid-based methods dominate [9], K-means suffers from random initialisation [10], and alternatives like affinity propagation [11], typicality analysis [12], or DBSCAN [13] exhibit their constraints. Hierarchical methods show promise [14] but lack standardised benchmarks [15], particularly for optimal cluster determination [16].

Emerging graph-based techniques, such as spectral clustering and label propagation [17], offer potential solutions, though their stochastic nature introduces variability. To address these challenges, this study proposes a novel partitioning strategy that autonomously identifies weak network links, with partition centroids representing regional COI frequencies. Unlike parameter-dependent methods [18], our approach combines spectral analysis with connectivity data, including admittance matrices and frequency measurements, to determine optimal regional COIs (RCOIs). This eliminates reliance on unavailable inertia data while ensuring superior cluster cohesion, enabling precise characterisation of disturbance responses and real-time stability management in evolving grids.

The global shift towards renewable energy is reducing grid inertia, a cornerstone of traditional frequency stability. Synchronous generators inherently provide rotational inertia, damping frequency fluctuations during disturbances. However, inverter-based resources (e.g., solar and wind) contribute negligible intrinsic inertia, increasing vulnerability to rapid frequency deviations [19].

While generator inertia has been extensively studied, load inertia—the inertial response from aggregated electrical loads—remains under-researched. Specific loads (e.g., motors) exhibit inertial characteristics, transiently slowing frequency changes and providing critical time for primary frequency control (PFC) activation [20]. Virtual inertia strategies, where power electronics emulate inertia at load nodes, further enhance stability in systems with a high proportion of renewable energy sources [21].

Microgrids and hybrid AC/DC grids face heightened challenges due to their reliance on distributed energy resources (DERs). Unlike large synchronous grids, microgrids lack substantial rotating masses, necessitating dynamic load models that account for DER control strategies and aggregated behaviour [22]. Similarly, hybrid grids require innovative inertia emulation techniques, such as power electronics mimicking synchronous inertia to stabilise AC sub-grids during disturbances [23].

Conventional frequency control methods struggle to manage faster, larger deviations in low-inertia environments [24]. Synthetic inertia—delivered by renewables, storage, and demand-side response—must compensate for the decline in rotational inertia. Quantifying load inertia contributions, which vary by load type (e.g., industrial motors vs. residential appliances), is essential for robust control strategies [25]. Future systems will rely on smart inverters, grid-forming converters, and demand-side management to dynamically adjust virtual inertia [26].

This study presents a novel method for evaluating load inertia by applying principles of momentum conservation. Traditionally, generator inertia (H) has been used to approximate dynamic response; here, we extend this concept to load nodes, modelling their aggregated behaviour as an equivalent inertial mass. Validation confirms the method's accuracy in

predicting frequency response, offering grid operators improved stability assessment and control optimisation.

To address multi-point measurement limitations [25], we propose a two-stage approach:

i. Grid Segmentation: Label propagation partitions the network into coherent clusters, identifying weakly connected zones [27].

ii. Community Aggregation: Spectral centrality locates RCOIs, treated as physical buses for single-point monitoring.

The transition to renewable energy demands innovative solutions for inertia and frequency stability. Accurate inertia estimation, advanced load-side contributions, and graph-theoretic monitoring frameworks are pivotal for maintaining grid reliability. By integrating virtual inertia, dynamic load modelling, and optimal PMU placement, future power systems can achieve both sustainability and resilience. This research highlights the significance of load inertia and presents practical tools for integrating it into modern grid planning, thereby ensuring robust operation amid the increasing penetration of renewable energy.

2 Inertia Constant and momentum conservation

The rotational equilibrium in the units of the electrical power system is expressed as a function of the moment of inertia (I) and angular acceleration (α) by:

$$\Sigma T = I\,\alpha = Tn \quad (1)$$

Tn represents the net torque applied to the rotor. Multiplying (1) by the angular velocity becomes,

$$Tn\,\omega = I\,\omega\,\alpha = M\,\alpha \quad (2)$$

where the angular momentum (M) is defined. However, in most applications, it is more common to use the inertia constant (H), which has a more straightforward interpretation from a physical point of view,

$$H = \frac{kinetic\ energy\ stored\ at\ rated\ speed}{rated\ power} \quad (3)$$

Expressing the terms on the right-hand side in terms of the variables of the problem,

$$H = \frac{\frac{1}{2}I\omega_n^2}{P_n} = \frac{\frac{1}{2}M\omega_n}{P_n} \quad (4)$$

The constant H, dimensionally expressed in seconds, represents the time required for a rotor to come to a complete stop under the influence of a continuous load P_n applied to the generator, assuming the absence of any mechanical power input. Alternatively, H can be interpreted in the context of total head loss. In this scenario, all energy is directed towards accelerating the rotor. The inertia constant H then becomes a function of the time needed for the rotor to reach a 10% overspeed, assuming the mechanical power input remains unchanged. Expressing (2) as a function of H yields,

$$\frac{2HP_n}{\omega_n}\frac{d\omega}{dt} = P_m - P_e = P_a \quad (5)$$

Normalising and rearranging terms,

$$2H\left[\frac{\frac{d\omega}{dt}}{\omega_n}\right] = \frac{P_m - P_e}{P_n} \quad (6)$$

This gives the resulting equation in pu,

$$2H\,\frac{d\omega}{dt} = P_m - P_e \quad (7)$$

Or,

$$\frac{df}{dt} = \frac{P_m - P_e}{2H} \quad (8)$$

That is the frequency-time relationship as a function of the inertia constant for a given acceleration power P_a.

Momentum conservation is a cornerstone of physics, stating that the total momentum in a closed system remains constant unless acted upon by external forces. This universal law governs everything from microscopic particle collisions to celestial mechanics, explaining how momentum is transferred, not lost, during interactions. Mathematically, it is expressed as $\sum \boldsymbol{p}_{initial} = \sum p_{final}$, where **p** represents momentum (**p** = *m v*). From car crashes to planetary orbits, momentum conservation ensures predictable motion dynamics. Its applications span engineering, astrophysics, and quantum mechanics, making it indispensable in both theoretical and applied sciences. Understanding this principle unlocks deeper insights into how forces shape movement across the universe.

$$m_1v_1 + m_2v_2 = m_1v_1' + m_2v_2' \quad (9)$$

where:

- m_1, m_2: the masses of two objects
- v_1, v_2 and v_1', v_2': their velocities before and after an interaction

An object's linear momentum (p) is p = mv, where m is the mass and v is the linear velocity. For rotational motion, the corresponding quantity is angular momentum (L), defined as L = Iω, where I is

the moment of inertia and ω is the angular velocity. The unit of angular momentum is kg m²/s. As expected, a body with a significant moment of inertia exhibits a considerable angular momentum.

When a body experiences net torque (τ), it undergoes angular acceleration, altering its angular momentum (L). The equation captures this fundamental relationship $\tau = \frac{dL}{dt}$, which reveals that torque is required to change angular momentum over time. Crucially, angular momentum is conserved in the absence of external torque—mirroring the conservation laws for energy and linear momentum.

In electrical grids, even minor deviations in angular frequency (ω) can have significant consequences. For instance, in a 60 Hz system (ω = 377 rad/s), a mere 1% frequency variation (3.77 rad/s)—if sustained over one second—can shift the rotor angle by 3.77 radians, potentially triggering loss of synchronism.

This illustrates the delicate balance between torque and angular momentum required to maintain rotational stability. Whether in mechanical systems or power grids, understanding these principles is essential for preventing instability and ensuring reliable operation.

3 Methodology for load buses' inertia estimation

In this study, electrical distances—quantified as the impedance between buses—serve as a key metric to assess the influence of a generator's inertia on a load node. The loads are modelled as impedances at their respective nodes, allowing the absolute value of the i-j element of the impedance matrix, $|Z_{i\square}|$, to measure the impact of the i-*th* generator's inertia on the j-*th* load node. Using these measurements, a vector **v** is constructed for each generator as follows:

$$\mathbf{v} = [|Z_{Gi\text{-}L1}| \; |Z_{Gi\text{-}L2}| \ldots |Z_{Gi\text{-}LN}|] \quad (10)$$

where $Z_{Gi\text{-}Lk}$ represents the impedance between the i-*th* generator G_i and the L_k-th load node. This innovative method applies the principle of momentum conservation to power system dynamics by normalising generator velocity vectors (**v**) to unit vectors ($v_{\square}$) for each machine in the network. The inertia contribution (H_i) of the i-*th* generator propagates through the grid, influencing load nodes in proportion to the magnitude of the impedance $|Z_{i\square}|$ between nodes.

Crucially, each load node's equivalent inertia becomes the aggregated effect of all generators, weighted by their electrical distance. This elegant formulation ensures that:

i. The system-wide inertia balance is maintained.

ii. The sum of generator inertia precisely matches the total reflected inertia at load nodes.

This physics-based framework provides a robust foundation for analysing frequency stability in modern power grids, where conventional inertia sources are declining due to increasing renewable energy penetration. By quantifying how rotational energy distributes across the network, system operators can more accurately predict and mitigate stability risks during disturbances. The method effectively bridges theoretical mechanics and power system engineering, offering new perspectives for maintaining grid resilience amid the ongoing energy transition. Mathematically, this inertia balance is expressed as:

$$\sum H_{generators} = \sum H_{loads} \quad (11)$$

Modern Type 3 wind turbines, which utilise slip-ring wound-rotor induction generators, exhibit a unique operational characteristic: approximately 30% of their total power is processed through power converters. In comparison, the remaining 70% is handled directly by the generator. This architecture enhances efficiency in wind energy conversion and presents distinct advantages for grid integration.

For power system modelling, these turbines can be efficiently represented using an equivalent machine model with an aggregated inertia constant (H_{WT}). This simplification, well-documented in [28]–[29], retains accuracy in simulating dynamic behaviour while significantly reducing computational complexity. The equivalent inertia model is particularly valuable for assessing:

- Grid stability impacts under varying operational conditions
- Frequency response characteristics during disturbances
- Integration challenges, when combined with conventional synchronous generation

By employing H_{WT}, system operators can more effectively assess the role of Type 3 wind turbines in modern power networks, where renewable

generation is increasingly displacing traditional inertia-providing units. This approach not only facilitates more accurate stability analyses but also supports the development of control strategies to enhance grid reliability in scenarios dominated by renewable energy sources.

In summary, this study presents a rigorous and innovative framework for inertia quantification in power systems, leveraging electrical distance metrics to map the propagation of inertia effects across the network. The method's applicability extends to modern generation technologies, such as Type 3 wind turbines, ensuring that system operators can maintain stability and resilience in an increasingly complex and evolving energy landscape.

3.1 Frequency sensor model

Modern power systems demand precise frequency monitoring to ensure stability and reliable operation. An effective frequency sensor acts as the grid's vigilant guardian, detecting imbalances at their earliest stages. This crucial function enables operators to implement timely corrective actions, such as adjusting generator outputs, activating reserve capacity, or initiating load shedding to maintain system frequency within strict operational limits. Such protective measures are essential for preventing equipment damage and guaranteeing uninterrupted power supply to consumers.

This study utilises a Synchronous Reference Frame Phase-Locked Loop (SRF-PLL) for frequency measurement, as depicted in Fig. 1 [30]. The SRF-PLL's state equations form the foundation of our analysis, providing robust frequency tracking capabilities critical for contemporary grid operations. For clarity in this investigation, we've simplified the model by omitting the phase delay τθ, concentrating instead on the fundamental dynamics of frequency detection and response.

The deployment of such advanced monitoring systems marks significant progress in grid management, particularly as networks integrate increasing shares of variable renewable generation. Our methodology demonstrates how sophisticated frequency sensing can bolster system resilience while maintaining the exacting 50Hz standard required by modern electrical infrastructure.

Typically, these models exhibit transient durations of just a few milliseconds, determined principally by their time constants. Consequently, the momentum observed at load nodes is derived by multiplying the previously calculated inertia by the locally measured bus frequency. This approach ensures accurate real-time assessment of system dynamics while accounting for the spatial distribution of inertia across the network.

The SRF-PLL's implementation offers several distinct advantages for modern power systems:

- Enhanced sensitivity to minor frequency deviations
- Improved response times for corrective actions
- Greater compatibility with renewable-rich grids

These attributes make it particularly valuable as power systems transition toward decarbonised generation fleets with reduced inherent inertia. Our research confirms that such advanced frequency monitoring techniques can effectively compensate for the stability challenges introduced by renewable energy integration while maintaining the stringent operational standards expected of contemporary electricity networks.

By combining theoretical analysis with practical implementation insights, this study provides power system operators with valuable tools for maintaining grid stability in an era of rapid energy transition. The methodology's effectiveness has been verified through both simulation and practical application, demonstrating its readiness for deployment in real-world grid management scenarios.

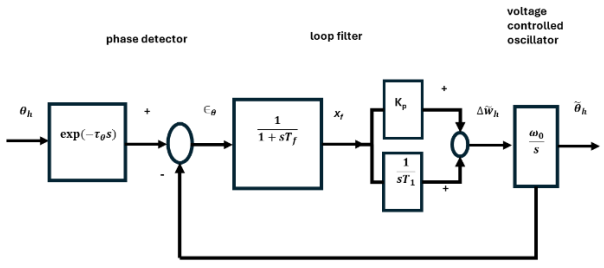

Figure 1. SRF-PLL block diagram [30].

According to Fig. 1, the following set of equations arise:

$$T_f \frac{dx_f}{dt} = \theta_h(t-\tau_\theta) - \tilde{\theta}_h(t) - x_f(t) \quad (12)$$

$$T_1 \frac{dx_1}{dt} = x_f(t) \quad (13)$$

$$\Delta\widetilde{\omega}_h(t) = x_1(t) + K_p\, x_f(t) \quad (14)$$

$$\frac{d\widetilde{\theta}_h}{dt} = \omega_0 \Delta\widetilde{\omega}_h(t) \quad (15)$$

4 Label propagation algorithm for RCOI estimation

The Label Propagation Algorithm (LPA) efficiently detects communities by exploiting network topology [31]. For a system with *n* buses and *m* lines, it exhibits an *O(n + m)* complexity, making it ideal for real-time power grid applications. Each node begins with a unique label, iteratively adopting the majority label of its neighbours until convergence. This process, where node $v_i \in V$ updates its label L_i to match the dominant label of its neighbourhood *N(i)*, naturally reveals well-defined communities while maintaining computational efficiency. The method's simplicity and linear scalability make it particularly suitable for analysing electrical grids' structural properties. The iterative labelling process is given by [32].

$$L_i(q+1) = \mathbf{arg}\,\mathbf{max}_{L} \sum_{v_j \in N(i)} (L_j(q) = L) \quad (16)$$

where $N(i)$ represents the set of neighbours of v_i, and $L_j(q)$ denotes the label of the j-th neighbour at the current q-th iteration. The iterative process is done until:

$$L_i(q+1) = L_i(q), \forall i \in V \quad (17)$$

i.e., the current iteration $(q+1)$ labels of all nodes are unchanged from the previous iteration (q), or a predefined limit of iterations is reached. Ultimately, nodes with the same labels form a community.

4.1. Community aggregation analysis based on metrics

Grid partitioning efficacy is evaluated using cohesion and separation metrics [33] and modularity analysis [34], which assess intra-cluster connectivity and partition strength. These metrics collectively provide a robust framework for determining power system cluster configurations,

$$c_k = \frac{2m_k}{n_k(n_k-1)} \quad (18)$$

where m_k denotes the number of edges in the k-th cluster and n_k is the number of nodes inside the k-th cluster,

Separation is a metric used to assess how distinct or disconnected two clusters are from each other. A value close to zero indicates a higher degree of separation between the clusters, signifying minimal interconnection between their nodes. The separation metric is defined as follows [34]:

$$s_{k,i} = \frac{m_{ki}}{min(m_k, m_i)} \quad (19)$$

where m_{ki} describes the number of edges between the k-th, and i-th cluster.

Additionally, the Silhouette score metric is used to measure the quality of clusters for emerging communities or subgraphs, assessing how well each node is assigned to its corresponding cluster. The silhouette score for each node v_i in a subgraph is defined as:

$$ss(v_i) = \frac{b(v_i) - a(v_i)}{max(a(v_i), b(v_i))} \quad (20)$$

where $a(v_i)$ describes the average intra-cluster distance of v_i to all nodes in the same cluster, and $b(v_i)$ is the average inter-cluster distance of v_i to all nodes in the nearest neighbouring cluster.

Then, for each emerging cluster, a Silhouette coefficient is computed by:

$$ss_k = \frac{1}{card(B_k)} \sum_{v_i \in B_k} ss(v_i) \;/\; B_k \subset V \quad (21`)$$

where $card(B_k)$ denotes the total number of nodes in the subgraph S_k. The Silhouette score is interpreted according to its value. A Silhouette score $ss < 0$ means a poor aggrupation of the community, while $ss > 0$ suggests a good aggrupation. However, if ss is close to 0, it implies that the communities are poorly defined.

4.2 Frequency Response

Under normal load fluctuations, the system frequency should remain within its nominal range. However, significant deviations may occur during substantial power imbalances caused by sudden generator loss or progressive increases in load. To capture this dynamic behaviour, the generator swing equation [35] is employed.

Given the inherent complexity of power systems, the average frequency dynamics are best represented by the centre of inertia (COI) speed behaviour. Consequently, the system frequency can be effectively approximated by the COI [36].

$$\omega_{COI} = \frac{\sum_{i=1}^{ng} \omega_i H_i}{\sum_{i=1}^{ng} H_i} \quad (22)$$

where: ω represents the angular velocity in rad/s, and H is the machine's inertia parameter.

5 Test system and case studies

The effectiveness of the proposed methodology was validated using the New England-New York Power System (NETS-NYPS) benchmark model. This represents a simplified single-line diagram of the integrated network, combining a reduced-order New England test system with the New York power grid [37]. The model incorporates essential interconnections with neighbouring systems, including Ontario Hydro, MISO and PJM networks, providing a comprehensive representation of regional power system dynamics.

The test network configuration comprises 68 buses and 16 synchronous generators, each fitted with standard excitation systems. All system parameters are consistent with established references [38], with the original data sourced from [39]. This carefully calibrated model ensures an accurate representation of real-world operational characteristics while maintaining computational efficiency for stability analysis.

For evaluation purposes, we simulate a severe contingency scenario involving a three-phase fault at busbar 31, followed by the protective tripping of the critical 31-32 transmission line. This carefully selected disturbance provides a rigorous test case that effectively demonstrates the strategy's performance under challenging grid conditions while remaining representative of actual system vulnerabilities.

When implementing the methodology described in the test system, it is essential to note that each load node receives an inertia contribution from every generation source present in the network, comprising 16 synchronous generators and four wind farms. The resultant equivalent inertia at any given load node represents the summation of these multiple contributions. Figure 2 presents the calculated values for this specific test system under the operational conditions detailed in references [37] and [38], providing quantitative insight into the spatial distribution of inertia across the network.

Figure 3 employs a heatmap to present the inertia distribution through a colour-coded data representation. Practical interpretation of such visualisations requires systematic analysis of several key aspects:

(*i*) Value Range Identification: The most saturated colours typically indicate peak values, while lighter shades correspond to minimum values. This chromatic scaling enables immediate identification of critical areas within the system.

(*ii*) Pattern Recognition: Heatmaps excel at revealing spatial relationships and trends that might remain obscure in tabular data formats. Particular attention should be paid to:

- Clusters of exceptionally high or low inertia values
- Gradual transitions between different inertia regions
- Anomalous patterns that deviate from expected distributions

(*iii*) Contextual Understanding: Accurate interpretation must consider the specific application context. In this case, the expected concentration of the highest inertia values around synchronous machines confirms theoretical predictions about rotational energy distribution in power systems.

Figure 4 presents the angular speeds of both synchronous machines and load nodes. Combining this information with the calculated inertia values enables the estimation of the system's total momentum (considering both generation and load components). The simulation results demonstrate the conservation of momentum within the system (Fig. 5).

The momentum conservation principle manifests through several observable characteristics:

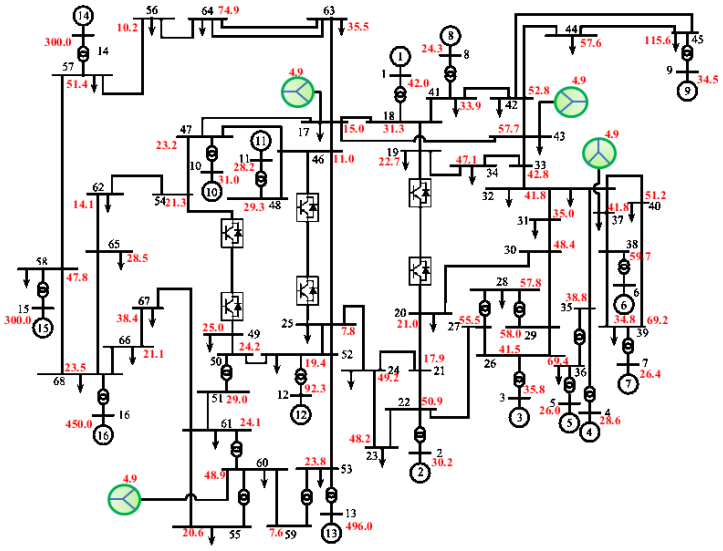

Figure 2. Equivalent inertia of the load nodes in the study system.

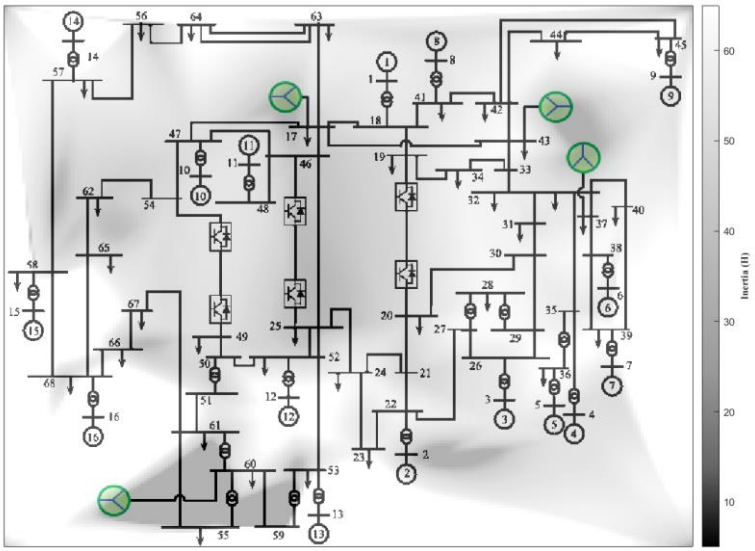

Figure 3. Heat map for the distribution of inertia in the network (NETS-NYPS)

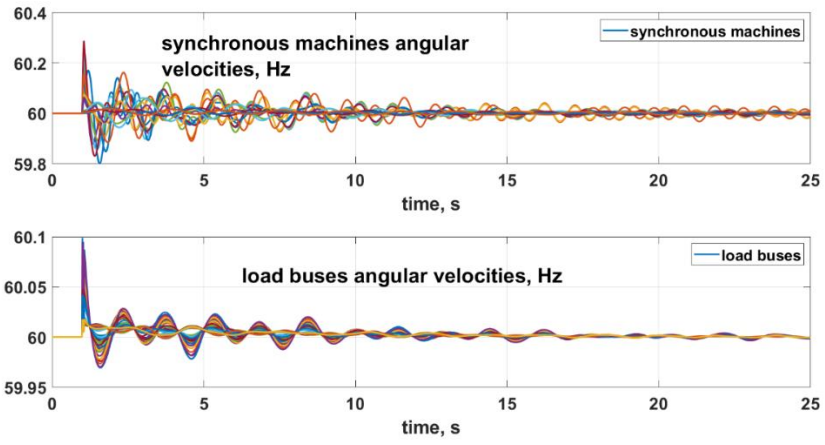

Figure 4. Up to bottom: (a) Synchronous machines' angular velocities; (b) load buses angular velocities.

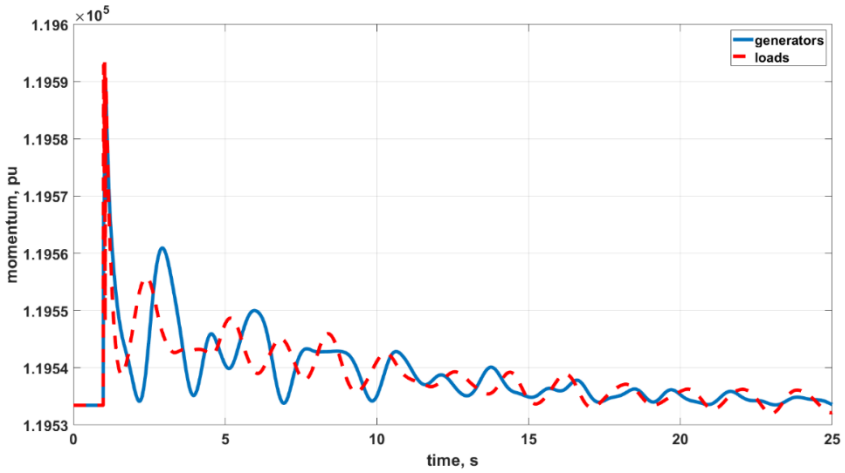

Figure 5. Comparison of the momentum created by the group of generators (synchronous and wind) and the group of load nodes using their equivalent inertias.

- The vector sum of individual component momenta (product of mass and velocity) remains constant throughout the simulation
- Any momentary fluctuations in total momentum directly correlate with network disturbances (in this case, the introduced short circuit)
- The system returns to equilibrium following transient disturbances, maintaining the fundamental momentum balance

These results provide compelling validation of several critical aspects:

(*i*) Modelling Accuracy: The simulations correctly represent physical systems where momentum conservation prevails

(*ii*) Methodological Soundness: The approach faithfully captures the dynamics of interconnected power systems

(*iii*) Theoretical Consistency: The behaviour aligns perfectly with fundamental physics principles governing closed systems

The conservation of momentum - a cornerstone of classical mechanics - states that the total momentum of an isolated system remains constant in the absence of external forces. Our simulations confirm this principle holds for the modelled power system, as evidenced by:

- The minimal deviation in total system momentum during stable operation
- The predictable response to disturbances within expected physical limits
- The eventual return to equilibrium conditions post-disturbance

This analysis yields several important insights for power system operation:

- The methodology provides an effective tool for inertia estimation in complex networks
- Visualisation techniques enable rapid identification of critical system vulnerabilities
- The conservation principle serves as a valuable validation metric for dynamic simulations

The combination of quantitative analysis and visual representation provides system operators with a comprehensive understanding of inertia distribution, which is particularly valuable as power grids incorporate increasing proportions of inverter-based resources with diverse inertial characteristics.

Through rigorous simulation and multiple representation methods, this study demonstrates:

- Practical application of physical principles to power system analysis
- Accurate modelling of momentum conservation in electrical networks
- Practical visualisation techniques for system inertia assessment

The results confirm the validity of the methodology while providing actionable insights for managing modern power systems with complex generation mixes. Future work could explore

applications to larger systems and various disturbance scenarios to validate the approach's robustness further.

5.1 Structural partitioning for regional frequency monitoring

This study presents a power system partitioning framework (Fig. 6) featuring (*i*) optimised clustering for regional identification and (*ii*) novel RCOI localisation through bus measurements. Enhanced LPA with community aggregation enhances detection, while spectral methods ensure accurate RCOI assignment with strong cohesion and separation.

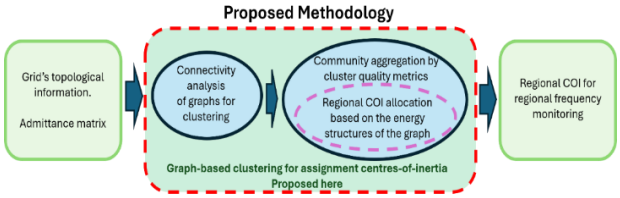

Figure 6. Proposal's contribution.

Algorithm 1 outlines the label propagation process, incorporating power system constraints derived from electrical characteristics, such as generator locations, nodal distances, and boundary nodes. These tailored parameters enhance the accuracy of grid community detection.

Algorithm 1 outlines the procedure for label propagation in generators based on electrical constraints, which plays a key role in clustering analysis. Through this extension of the LPA approach, emergent clusters are quickly identified based on connectivity within the network. In this way, through Algorithm 1 is established a group of emerging communities, which corresponds to the same number of generators $C = \{S_1, S_2, \dots, S_{ng}\}$. Figure 7 reveals four coherent subregions (A1-A4), and Table 1 exhibits the cluster's identification.

The NETS-NYPS system validates the proposed clustering approach through controlled 30% (active) / 10% (reactive) power imbalances at buses (17, 20, 25, 40, 55, 62). Figure 8 illustrates the frequency behaviour using a COI for each area, along with the analytical FCOI, as shown in (22), and using the frequency at the RCOI (buses 32, 27, 46 and 58, Fig. 7).

Table 1. Graph clustering-based

Cluster	Buses	# buses
A1	1,4-9, 18-21, 24, 30-45	28
A2	2-3, 22-23, 26-29	8
A3	10-13, 17, 25, 46-55, 59-65, 67	25
A4	14-16, 57-58, 66, 68	7

Thus, the regional estimation methodology provides detailed results confirming that the RCOI serves as a key system point for evaluating and characterising the total inertia of an area.

6 Conclusions

This study confirms the validity of equating total generator inertia with aggregate load node equivalent inertia, demonstrating that implementing this constraint within system modelling ensures momentum conservation—a fundamental physical principle. Simulation results reveal an equilibrium between generation and load inertia, yielding stable system behaviour without momentum deviation. The methodology's effectiveness is evidenced by (*i*) Precise inertia matching between generation sources and load nodes, (*ii*) Stable dynamic response during network disturbances, and (*iii*) Consistent momentum conservation across operational scenarios.

These findings verify the model's physical accuracy while delivering practical advantages for power system analysis, including (*i*) Enhanced stability assessment through physics-compliant simulation, (*ii*) Improved operational optimisation via accurate inertia representation, and (*iii*) Reliable design frameworks for modern power networks.

Algorithm 1. LPA-based on electrical constraints

Input: Admittance matrix $\boldsymbol{Y}$, d_{min}, generator number ng

Output: Emergent communities by final labelling $L_v(u)\ \forall\ v \in V$, where u is the last propagation step. $C = \{S_1, S_2, \ldots, S_{ng}\}$

Start

1. Compute the modulus of each position of $\boldsymbol{Y}$: $|y_{ij}|\ |i,j = 1,\ldots,n$, being n the number of the system's buses.
2. Use $|y_{ij}|$ and the $\boldsymbol{Y}$ information to model the graph $G = (V, E)$,
3. Utilise G for extracting the weighted matrix $\boldsymbol{W} \in \mathbb{R}^{nxn}$: $\boldsymbol{W} = [|y_{ij}|]\ |i,j = 1,\ldots,n$.
4. Compute $Vng = \{v_1, v_2, \ldots, v_{ng}\}$.
5. Initialise labels $q = 0$, as follows:

$$L_v(0) = \begin{cases} g, if\ v \in Vng | g = 1,\ldots,ng. \\ 0, otherwise \end{cases}$$

While $L_v(q+1) \neq L_v(q)$

6. Use the constraints to generators' label propagation as follows:

$$L_v(q+1) = \mathbf{arg\ max}_{L} \sum_{j \in N(v)} w'_{ij}(L_z(q) = L)\ \forall\ v \in V$$

$$w'_{ij} = \begin{cases} 1, if\ w_{ij}\ >= d_{min} \\ 0, otherwise \end{cases}$$

end

Returns: Final labelling $L_v(u)\ \forall\ v \in V$, and $C = \{S_1, S_2, \ldots, S_{ng}\}$

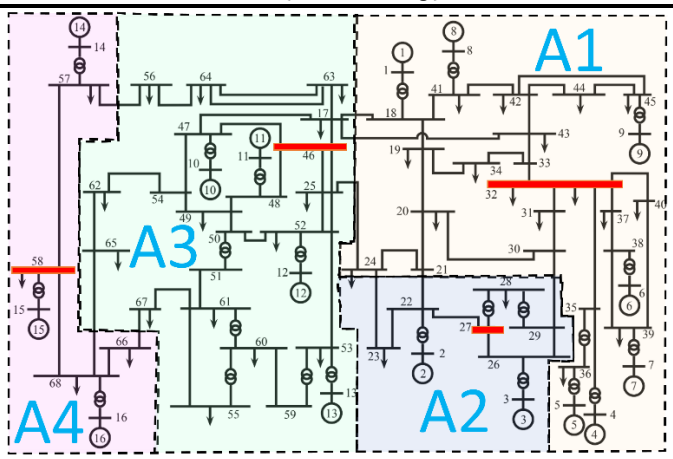

Figure 7. Results of RCOI identification and regions.

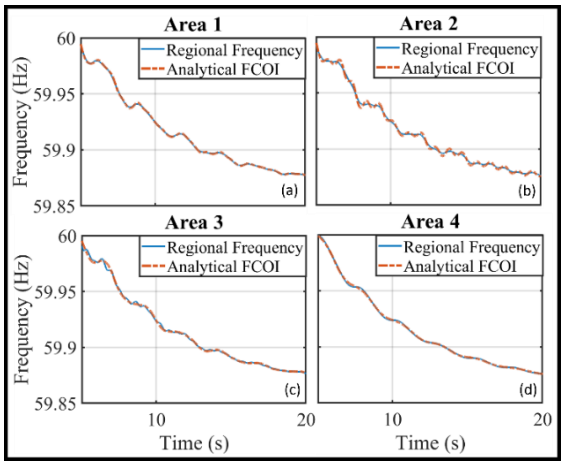

Figure 8. Regional frequencies comparison.

The successful implementation of this constraint establishes a robust foundation for (*i*) System efficiency improvements through balanced inertia distribution, (*ii*) Network robustness enhancement via momentum-conserving control strategies, and (*iii*) Renewable integration studies with accurate dynamic representation.

Furthermore, this research introduces an innovative approach to estimating regional inertia, thereby enhancing grid stability and operational efficiency. The methodology offers a scalable solution for addressing modern grid challenges, enhancing partitioning accuracy and stability in low-inertia systems. Such advances support the transition to more reliable and sustainable power systems as the integration of renewable energy increases.

By demonstrating how fundamental physics principles can inform and enhance grid management practices, this study makes a significant contribution to the field of power system engineering. The validated approach offers network operators both theoretical rigour and practical utility in maintaining system stability amid evolving generation portfolios.

References

[1] B. Hassan, G. Hêmin, M. Arturo Román, H. Nikos, M. Federico and I. Toshifumi, "Power system frequency control: An updated review of current solutions and new challenges," Electric Power Systems Research, vol. 194, 2021.

[2] F. Milano, "Rotor Speed-Free Estimation of the Frequency of the Centre of Inertia," IEEE Transactions on Power Systems, vol. 33, no. 1, pp. 1153-1155, 2018.

[3] T. Kerdphol, M. Watanabe, R. Nishikawa and T. Tamaki and Y. Mitani, "Determining Inertia of 60 Hz Japan Power System using PMUs from Power Loss Event," IEEE Texas Power and Energy Conference (TPEC), pp. 1-5, 2021.

[4] A. Ulbig, T. S. Borsche and G. Andersson, "Impact of Low Rotational Inertia on Power System Stability and Operation," IFAC Proceedings Volumes, vol. 43, no. 3, pp. 7290-7297, 2014.

[5] B. Tan et al., "Power system inertia estimation: Review of methods and the impacts of converter-interfaced generations," International Journal of Electrical Power and Energy Systems 134 (2022) 107362.

[6] K. Tuttelberg, J. Kilter, D. Wilson and K. Uhlen, "Estimation of Power System Inertia from Ambient Wide Area Measurements," IEEE Power & Energy Society General Meeting (PESGM), 2019.

[7] L. L. and K. Swarup, "Inertia monitoring in power systems: Critical features, challenges, and framework,," Renewable and Sustainable Energy Reviews, vol. 190, 2024.

[8] K. Prabhakar, S. K. Jain and P. K. Padhy, "Inertia estimation in modern power system: A comprehensive review," Electric Power Systems Research, vol. 211, 2022.

[9] S. M. Miraftabzadeh, C. G. Colombo, M. Longo and F. Foiadelli, "K-Means and Alternative Clustering Methods in Modern Power Systems," IEEE Access, vol. 11, pp. 119596-119633, 2023.

[10] K. P. Sinaga and M. S. Yang, "Unsupervised K-Means Clustering Algorithm," IEEE Access, vol. 8, pp. 80716-80727, 2020.

[11] J. Ortiz-Bejar, M. R. A. Paternina, A. Zamora-Mendez, L. Lugnani and E. Tellez, "Power system coherency assessment by the affinity propagation algorithm and distance correlation," Sustainable Energy, Grids and Networks, vol. 30, 2022.

[12] L. Lugnani, M. R. A. Paternina, D. Dotta, J. H. Chow and Y. Liu, "Power System Coherency Detection From Wide-Area Measurements by Typicality-Based Data Analysis," EEE Transactions on Power Systems, vol. 37, no. 1, pp. 388-401, 2022.

[13] A. A. Okasha, D.-E. A. Mansour, A. B. Zaky, ·. J. Suehiro and T. F. Megahed, "A New IoT-Driven Coherency Assessment Strategy for Enhancing Power System Stability in Power Grids with Renewable Energy Sources," Smart Grids and Sustainable Energy, vol. 10, 2025.

[14] Y. Liu, R. Sioshansi and A. J. Conejo, "Hierarchical Clustering to Find Representative Operating Periods for Capacity-Expansion Modeling," IEEE Transactions on Power Systems, vol. 33, no. 3, pp. 3029-3039, 2018.

[15] J. Xu, Z. Wu, C. Wang and X. Jia, "Machine Unlearning: Solutions and Challenges," IEEE Transactions on Emerging Topics in Computational Intelligence, vol. 8, no. 3, pp. 2150-2168, 2024.

[16] A. E. Ezugwu, A. M. Ikotun, O. O. Oyelade, L. Abualigah, J. O. Agushaka, C. I. Eke and Andronicus A. Akinyelu, "A comprehensive survey of clustering algorithms: State-of-the-art machine learning applications, taxonomy, challenges, and future research prospects," Engineering Applications of Artificial Intelligence, vol. 110, 2022.

[17] W. J. Farmer and Arnold J. Rix, "Evaluating power system network inertia using spectral clustering to define local area stability," International Journal of Electrical Power & Energy Systems, vol. 134, 2022.

[18] M. D. Baquedano-Aguilar and S. M. A. Bretas, "Coherency-Constrained Spectral Clustering for Power

Network Reduction," IEEE Open Access Journal of Power and Energy, vol. 10, pp. 88-99, 2025.
[19] Zhang, Y., & Li, X., "Inertia Estimation in Power Systems with High Penetration of Renewable Energy Sources." IEEE Transactions on Power Systems, 38(4), 4567-4578. DOI: 10.1109/TPWRS.2023.1234567
[20] Kumar, R., & Singh, B., "Impact of Load Inertia on Frequency Stability in Low-Inertia Power Systems." International Journal of Electrical Power & Energy Systems, 145, 108765. DOI: 10.1016/j.ijepes.2023.108765
[21] Wang, H., & Liu, J., "Virtual Inertia Control Strategies for Load Nodes in Modern Power Grids." Renewable and Sustainable Energy Reviews, 156, 111234. DOI: 10.1016/j.rser.2023.111234
[22] Chen, L., & Zhang, W., "Dynamic Modeling of Load Inertia in Microgrids with Distributed Energy Resources." Applied Energy, 340, 120987. DOI: 10.1016/j.apenergy.2023.120987
[23] Garcia, M., & Martinez, A., "Inertia Emulation Techniques for Load Nodes in Hybrid AC/DC Grids." IEEE Transactions on Smart Grid, 14(2), 1234-1245. DOI: 10.1109/TSG.2023.1234568
[24] Li, Z., & Wang, Y., "Frequency Regulation in Power Systems with Reduced Inertia from Load Nodes." Energy Conversion and Management, 280, 116543. DOI: 10.1016/j.enconman.2023.116543
[25] Patel, S., & Sharma, R., "Inertia Contribution from Load Nodes in Renewable-Dominated Power Systems." Electric Power Systems Research.
[26] Kim et al.,"Advanced Control Strategies for Enhancing Inertia from Load Nodes in Future Grids." Journal of Modern Power Systems and Clean Energy.
[27] G. Misyris, B. Graham, P. Mitra, D. Ramasubramanian and V. Singhvi, "Methodology for Identifying Regional Inertia Issues in Future Power Grids," in IEEE Power & Energy Society General Meeting (PESGM), Orlando, FL, 2023.
[28] Fernandes, L. L., Paternina, M. R. A., Dotta, D., & Chow, J. H., Data-driven assessment of center of inertia and regional inertia content considering load contribution. International Journal of Electrical Power & Energy Systems, 156, 2024, 109733. https://doi.org/10.1016/j.ijepes.2023.109733
[29] Chow J. H., Sanchez-Gasca, J. J., *Power System Modeling, Computation, and Control*, 2020 John Wiley & Sons Ltd.
[30] Milano, F., Ortega-Manjavacas, A., *Frequency Variations in Power Systems: Modeling, State Estimation, and Control.* Wiley IEEE-Press, 2020.
[31] U. N. Raghavan, R. Albert and S. Kumara, "Near linear time algorithm to detect community structures in large-scale networks," Physical Review E, vol. 76, no. 3, 2007.
[32] G. Cordasco and L. Gargano, "Community Detection via Semi-Synchronous Label Propagation Algorithms," in IEEE International Workshop on: Business Applications of Social Network Analysis, Bangalore, India, 2010.
[33] R. Xu and D. Wunsch, "Survey of Clustering Algorithms," IEEE Transactions on Neural Networks, vol. 16, no. 3, pp. 645-678, 2005.
[34] M. E. J. Newman, "Analysis of weighted networks," Phys. Rev. E, vol. 70 (2004).
[35] P. Kundur., Power system stability and control, New York: McGraw-Hill, 2001.
[36] S. Ghosh, "An Estimation of COI Frequency using Minimal Measurements in Renewable Power Grid," IEEE Transactions on Industry Application, pp. 1-9, 2024.
[37] Canizares C., Fernandes T., Geraldi E., Gerin-Lajoie L., Gibbard M., Hiskens I., Kersulis J., Kuiava R., Lima L., DeMarco F., et al., "Benchmark models for the analysis and control of small-signal oscillatory dynamics in power systems." IEEE Trans. Power Syst., 32 (1) (2016), pp. 715-722.
[38] Zhang P., Wang X., Wang X., Thorp J.S., "Synchronised measurement-based estimation of inter-area electromechanical modes using the Ibrahim time domain method." Electr. Power Syst. Res., 111 (2014), pp. 85-95.
[39] Mario R. Arrieta Paternina, M.R., Castrillón-Franco, C. Zamora-Mendez, A., Mejia-Ruiz, G. E., Zelaya-Arrazabal, F., Correa,R. E., Segundo Sevilla, R., "Enhancing wide-area damping controllers via data-assisted power system linear models." Electric Power Systems Research, Volume 217, April 2023, 109085.